Some recent developments in the chemical synthesis of inorganic nanotubes

Yujie Xiong, Brian T. Mayers and Younan Xia*

Received (in Cambridge, UK) 14th July 2005, Accepted 18th August 2005
First published as an Advance Article on the web 21st September 2005
DOI: 10.1039/b509946c

Inorganic nanotubes have been a subject of intensive research in the past decade. We recently developed a number of synthetic strategies for generating nanotubes from inorganic materials that do not have a layered structure. It is the intention of this contribution to provide a brief account of these research activities.

Introduction

The discovery of carbon nanotubes (CNTs) in 1991 by Iijima[1] opened an exciting field of research for both nanoscience and nanotechnology. Because of their potential use in applications related to hydrogen storage and fabrication of field-emission displays, transistors, diodes, sensors, and actuators,[2] synthesis and characterization of CNTs have been actively pursued by many groups in the past 14 years. As to their structures, CNTs can be described as single or multiple concentric cylinders of graphitic sheets with both ends closed due to the presence of five-membered rings.[3] To date, CNTs have been successfully synthesized using a variety of methods, with notable examples including arc discharging,[4] laser vaporization,[5] hydrocarbon pyrolysis, and chemical vapor deposition (CVD).[6]

Similar to graphite, solid materials such as WS_2 and MoS_2 also feature a layered structure, in which the atoms are covalently bonded to form two-dimensional layers that are stacked together through van der Waals interactions.[7] Under appropriate conditions, the two-dimensional sheets can also be rolled up to form seamless nanotubes. Since the report of WS_2 nanotubes in 1992 by Tenne,[8] inorganic nanotubes have been synthesized from a wealth of layered compounds, including MoS_2,[9] BN,[10] VO_x,[11] $NiCl_2$,[12] $NbSe_2$,[13] ZrS_2,[14] HfS_2,[14]

Department of Chemistry, University of Washington, Seattle, WA 98195-1700, USA. E-mail: xia@chem.washington.edu; Fax: (+1)206-685-8665; Tel: (+1)206-543-1767

Yujie Xiong

Yujie Xiong was born in Jiangxi, China in 1979. He entered the Special Class for the Gifted Young (SCGY) at the University of Science and Technology of China (USTC) in 1996, and received a BSc in chemical physics in 2000. He received a PhD in inorganic chemistry from the USTC (with Prof. Yi Xie) in 2004. He joined Prof. Younan Xia's group at the University of Washington in Seattle as a postdoctoral fellow in 2004. His current research interests include solution-phase synthesis, self-assembly, nucleation and growth, and surface plasmonic properties of nanostructured materials.

Brian T. Mayers

Brian T. Mayers was born in Bronx, NY, in 1976. He obtained a BA degree in chemistry and computer science from Wesleyan University (Middletown, CT) in 1998. He received an MSc degree from the University of Washington in 2002 and a PhD degree in organic and materials chemistry (with Prof. Younan Xia) from the University of Washington in 2003. He is working as a postdoctoral fellow in the Department of Chemistry and Chemical Biology at Harvard University (with Prof. George M. Whitesides).

Younan Xia

Younan Xia was born in Jiangsu, China in 1965. He received a BSc in chemical physics from the University of Science and Technology of China (USTC) in 1987. He received an MSc degree in inorganic chemistry from the University of Pennsylvania (with Prof. Alan G. MacDiarmid) in 1993, and a PhD degree in physical chemistry from Harvard University (with Prof. George M. Whitesides) in 1996, after which he stayed at Harvard and worked as a postdoctoral fellow with Prof. George M. Whitesides and Prof. Mara Prentiss. In 1997, he started as an Assistant Professor of Chemistry at the University of Washington. He was promoted to the rank of Professor in 2003. His research interests include nanostructured materials, self-assembly, photonic crystals, colloidal chemistry, surface functionalization, electrospinning, microfabrication, conjugated polymers, microfluidic and microanalytical systems, and novel devices for photonics, optoelectronics, and displays.

NbS_2,[15] and TaS_2.[15] Both vapor- and solution-phase methods could be applied to the production of these nanotubes. It was suggested that the rolling-up process could only occur on the layers with an inherent ability to bend and fold.[10,16]

Synthesis of nanotubes from inorganic materials that do not have a layered crystal structure has also attracted considerable attention because nanomaterials with such a morphology may find unique applications in areas such as catalysis, electronics, photonics, information storage, optoelectronics, and sensing. Compared with layered compounds, formation of nanotubes from other solid materials requires much more effort to bring together atoms or small particles into hollow cylinders in the process of crystallization. As a result, production of nanotubes from non-layered materials often requires the use of templates such as CNTs, nanowires, and porous membranes. Rolling of thin films due to residual stress has also been demonstrated to fabricate inorganic tubes with micrometer-sized openings.[17] Also, the relief of strain in the transformation from bilamellar structures to unilamellar sheets could drive the formation of tubular structures.[18] To date, nanotubes have been synthesized from a broad range of non-layered inorganic materials, with examples including SiO_2,[19] TiO_2,[19] Al_2O_3,[20] In_2O_3,[21] Ga_2O_3,[21] GaN,[22] CdS,[23] CdSe,[23] ZnS,[24] Au,[25] Co, and Fe.[26] Some of these syntheses still need to be greatly improved in terms of yield, purity, crystallinity, uniformity, as well as control over both dimension and composition.

The present feature article reviews our own contributions to the synthesis of nanotubes from inorganic materials that do not contain the layered structure. We explicitly describe three different approaches to fabrication of tubular nanostructures. Each approach is highlighted by at least one example. In the first approach, nucleation-induced concentration depletion at the surface of a seed is used to generate tellurium nanotubes with controllable dimensions. In a second approach, physical and chemical templating procedures are applied to synthesize nanotubes from various kinds of semiconductors and metals, with Se and Ag nanowires serving as two typical examples of templates. Finally, we demonstrate the fabrication of ceramic hollow nanofibers by electrospinning. It is believed that the techniques described here can also be extended to a broader range of materials. By the end of this article, we also briefly discuss the potential extension of these synthetic strategies to hollow nanostructures with dimensionality other than one, as well as some new potential applications associated with these inorganic nanotubes.

Concentration depletion method

Many solid materials exhibit a one-dimensional growth habit as a result of the inherently anisotropic feature in their crystal lattices. Trigonal-phase selenium (*t*-Se) and tellurium (*t*-Te) are two such examples. They share the same crystal structure (see the upper left inset of Fig. 1a), in which the atoms are covalently linked into helical chains and then packed into a hexagonal lattice through van der Waals interactions. The bonding between atoms is therefore much stronger along the *c*-axis than in the directions perpendicular to it. Dictated by this anisotropy in interaction, these two solids easily grow as uniform nanorods and nanowires from a solution-phase.

By forming a concentration depletion zone at the surface of a growing seed, both *t*-Se and *t*-Te can be directed to grow into nanotubes. The simplest way for achieving concentration depletion in a solution-phase is to reduce the formation rate of atoms. When this rate is sufficiently slow, the concentration of atoms in the solution will be reduced to zero right after a homogeneous nucleation event. This so-called ''nucleation-induced concentration depletion'' was first observed in various colloidal systems by Matijević in 1994.[27] A similar observation was also reported by Whitesides and co-workers when they were growing calcite crystals on gold surfaces patterned with fine grids of self-assembled monolayers.[28] In general, a concentration depletion zone will develop on the surface of a seed when the supply and mobility of atoms in the solution are low while the crystal growth rate is very high. As atoms in solution approach the crystal, they are immediately consumed and bound to the edges of a growing seed, because these sites usually have higher free energies than other regions on the surface.[29] As a result, a zone of complete concentration depletion is formed in the center of the growing surface.

As a case study, the polyol process was demonstrated by us to produce *t*-Te nanotubes, in which ethylene glycol served as both solvent and reducing reagent and orthotelluric acid was used as a precursor to the Te atoms.[30] Owning to the highly anisotropic interactions in *t*-Te (Fig. 1a, the upper left inset),

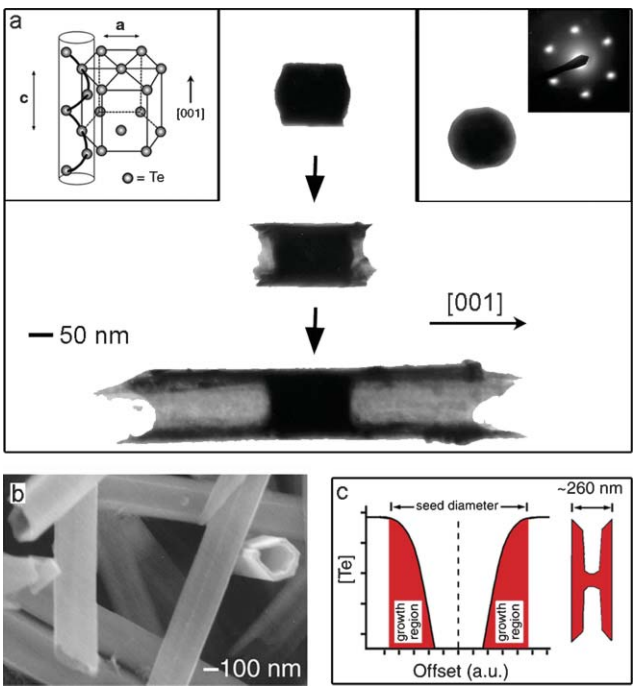

Fig. 1 (a) TEM images of *t*-Te nanotubes at three different stages of growth. The inset at the upper left corner shows an illustration of the crystal structure of *t*-Te that contains helical chains of Te atoms packed parallel to each other along the *c*-axis. The inset at the upper right corner gives a cross-sectional TEM image of a cylindrical seed, together with a micro-diffraction pattern obtained by focusing the electron beam onto this seed along the *c*-axis. (b) SEM image of *t*-Te nanotubes prepared using the concentration depletion method. (c) Concentration profile (side view) of Te atoms at the growing end of a seed. Adapted from ref. 30, © 2002 Wiley-VCH. Used with permission.

the growth direction of this material is confined to the <001> axis and the single-crystal seeds often end up in a cylindrical shape. The preferential growth direction has been confirmed by electron diffraction (see the upper right inset for a typical pattern). The key component of this synthesis is orthotelluric acid, a precursor that allows for an easy and tight control over the concentration of Te atoms in the solution. Orthotelluric acid has to be decomposed into TeO_2 before it can be further reduced by ethylene glycol to form Te atoms. Therefore, this reaction can only produce Te atoms at a very slow rate. The simultaneous formation of many seeds *via* the homogeneous nucleation process will reduce the concentration of Te atoms to an extremely low level. In other words, the decomposition reaction of orthotelluric acid serves as a rate-determining step to control the concentration of Te in the solution-phase. After the nucleation step, further addition of Te atoms to the seed should preferentially occur at the circumferential edge of each cylindrical seed. Subsequent transport of Te atoms to the fast growing edge will lead to complete depletion of Te atoms in the central portion of the {001} surface, and eventually result in the formation of single-crystal nanotubes with a uniform, well-defined cross-section (see Fig. 1b for the SEM image of a typical sample). The entire growth process as a function of time can also be appreciated from the TEM images in Fig. 1a.

In the concentration depletion method, the concentration of atoms is the key parameter to control if one wants to vary the diameters of the tubes. In the case of tellurium, as the initial concentration of orthotelluric acid was reduced, the lateral dimensions of the cylindrical seeds decreased. On the other hand, the wall thickness of the nanotube was far less sensitive to the variation of concentration of orthotelluric acid, because this value was mainly determined by the diffusion length scale of Te atoms on the surface of a seed.[31] Fig. 1c illustrates the concentration distribution profile of Te atoms at the growing surface of a seed, where the shaded regions correspond to the lateral diffusion zones of Te atoms. As the diffusion length became comparable to the radius of the cylindrical seed, the final product was found to evolve from nanotubes into solid nanorods. This change from a tube to a rod morphology also implies that the concentration depletion model is a reasonable one, accounting for the growth of *t*-Te nanotubes. This soft, solution-phase method is believed to be potentially extendable to other inorganic materials (*e.g.*, *t*-Se[32] and Sb_2S_3[33]) containing chain-like building blocks.

Template-directed approach

Templating against existing nanostructures (*e.g.*, wires, rods, belts, and channels) represents a straightforward and powerful route to nanostructures with hollow interiors. The template simply serves as a scaffold around which a different material is generated *in situ* and directed to grow into a nanostructure with its morphology complementary to that of the template.[34] To this end, many different strategies have been successfully demonstrated. In one approach, it has been shown that some single-crystal nanostructures can serve as substrates for the epitaxial growth of another solid to obtain coaxial nanocables containing sharp structural and compositional interfaces.[35] By varying the composition of reactant gas, it is also feasible to generate multiple-sheath nanocables *via* epitaxial growth in a layer-by-layer fashion.[36] In a second approach, the surfaces of nanowires can be directly coated (using a vapor- or solution-phase method) with conformal sheaths made of a different material (usually amorphous or polycrystalline in structure) to generate coaxial nanocables.[37] Selective removal of the wires will lead to the formation of nanotubes with well-controlled inner and outer diameters. In a third approach, which is often referred to as a ''template-engaged'' process, nanowires are reacted with appropriate chemical reagents under carefully controlled conditions to be partially or completely converted into another material without changing the morphology.[38] All these routes can be applied to fabricate inorganic nanotubes, with the first two commonly known as ''physical templating'' and the last one as ''chemical templating''. Here we only focus on some recent demonstrations from our own group.

Physical templating

Fig. 2a shows a schematic of physical templating. The first step involves the deposition of a desired material on the surface of template. In the second step, the template is selectively removed to form nanotubes. Two types of templates have been explored in our work: Ag nanowires with a pentagonal cross-section and *t*-Se nanowires with a triangular cross-section. The Ag nanowires were synthesized *via* a modified polyol process, in which $AgNO_3$ was reduced by ethylene glycol in the presence of poly(vinyl pyrrolidone) (PVP).[39] Coating of these Ag nanowires with amorphous silica was achieved using a sol-gel approach, or the so-called ''Stöber method'', which has been extensively exploited to form uniform coatings on nanoparticles of metals and metal

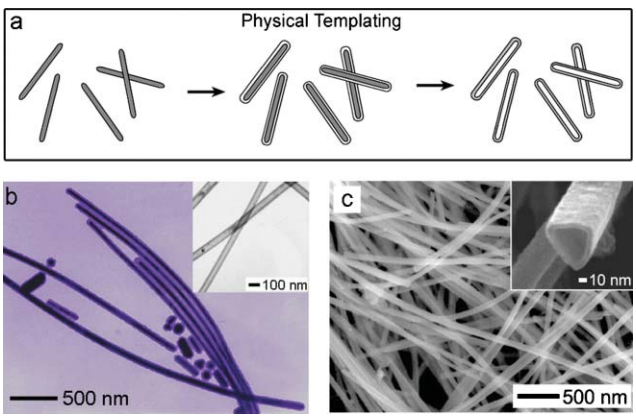

Fig. 2 (a) Schematic illustration of a physical templating process, where core-sheath structures are formed as the initial product by coating the surfaces of nanowires with a new material. Removal of the template leads to structures with hollow interiors. (b) TEM image of Ag–SiO_2 nanocables that were synthesized with Ag nanowires as a physical template. The inset shows a TEM image of silica nanotubes after selective removal of Ag. Adapted from ref. 42, © 2002 American Chemical Society. Used with permission. (c) SEM image of Pt nanotubes that were prepared by coating *t*-Se nanowires with Pt, followed by dissolution of Se wires in hydrazine monohydrate. The inset is an SEM image clearly showing the triangular cross-section of a Pt nanotube. Adapted from ref. 45, © 2003 American Chemical Society. Used with permission.

oxides.[40] For metal surfaces such as gold and silver, a primer (*e.g.*, amine- or mercapto-terminated siloxane) is needed in order to generate a homogeneous, conformal coating.[41] In our approach, Ag nanowires were dispersed in a mixture of 2-propanol and water, and formation of the SiO_2 coating involved the ammonia-catalyzed hydrolysis of tetraethylorthosilicate (TEOS) and subsequent condensation of SiO_2 sols onto the surface of Ag nanowires. Using this procedure, the SiO_2 could be directly applied as an amorphous coating on the Ag wire without the use of any primer.[42] Fig. 2b shows a TEM image of the resultant Ag–SiO_2 nanocables. The thickness of the SiO_2 sheaths could be readily controlled by changing the reaction time and/or the concentration of the precursor solution. In the late stage of the coating process, the ammonia also attacked the Ag nanowires through the following reaction:

$$4Ag + O_2 + 8NH_3{\cdot}H_2O \rightarrow 4Ag(NH_3)_2^+ + 4OH^- + 6H_2O$$

Thus SiO_2 nanotubes could be obtained by keeping the as-prepared sample of Ag–SiO_2 nanocables in an ammonia solution for 1 day. The inset of Fig. 2b shows a typical TEM image of the as-synthesized SiO_2 nanotubes. Compared with the nanotubes (made of SiO_2 or other metal oxides) prepared by templating against polymer nanofibers or CNTs,[43] both the length and wall thickness of the nanotubes prepared using this method could be easily controlled, and the nanostructures were also characterized by relatively smooth surfaces and better mechanical strength, thanks to the slow and complete condensation of SiO_2 sols.

t-Se nanowires can be synthesized using a chemical or sonochemical method.[44] They are characterized by a triangular cross-section as dictated by their hexagonal crystal structure. These nanowires were found to be superior for the deposition of Pt sheaths. The formation of the Pt coating could be achieved by reducing $PtCl_2$ in an alcohol solution.[45] Two reduction reactions might be involved in the conformal coating of *t*-Se nanowires with Pt sheaths: *i*) the initial reduction of the Pt(II) salt by the *t*-Se template itself at the interface;[46] and *ii*) the reduction of the Pt(II) salt by an alcohol, which also served as the solvent.[47] The reduction of Pt(II) by Se(0) could continue until the surface of a *t*-Se nanowire was completely covered. Subsequent deposition of the Pt was dominated by the alcohol reduction. The Pt layer could continue to grow until the reaction was quenched or all of the Pt(II) salt had been consumed. After Pt coating, the *t*-Se template could be easily removed to yield nanotubes using chemical or thermal methods. For example, the *t*-Se template could be selectively dissolved in pure hydrazine monohydrate.[46] The key here is to remove excess Pt(II) salt before the dissolution of template, avoiding the formation of additional Pt particles by hydrazine reduction. Another effective way is to evaporate the *t*-Se template at 200–250 °C, thanks to the low melting point and high vapor pressure of selenium. Fig. 2c shows a typical SEM image of Pt nanotubes produced using this approach. Note that the triangular cross-section of the *t*-Se template was faithfully duplicated by the Pt nanotubes, which was supported by SEM (inset of Fig. 2c). Since the thickness of the Pt coating was not dependent on the dimensions of the Se template, the Pt nanotubes could potentially be grown to any thickness by controlling reaction time and/or the concentration of the Pt(II) salt.

Chemical templating

Different from physical templating, chemical templating usually involves some reactions between the template and a precursor to form the desired material. Fig. 3a shows a schematic outline of the procedure that generates chalcogenide nanotubes by chemically templating against *t*-Se nanowires. In the case of CdSe,[48] when *t*-Se nanowires were added to an aqueous medium containing Cd^{2+} cations and then refluxed, elemental Se disproportionated into Se^{2-} and SeO_3^{2-} anions.[49] The Se^{2-} anions combined with the Cd^{2+} cations to generate insoluble CdSe nanoparticles that deposited *in situ* as a conformal sheath around each *t*-Se nanowire. Some $CdSeO_3$ nanoparticles might also decorate the surface of resultant Se–CdSe nanocables, and they could be dissolved in hot water. The unreacted core of *t*-Se could be removed through thermal evaporation. Fig. 3b shows a typical TEM image of the as-synthesized CdSe nanotubes. With *t*-Se nanowires as chemical template, metal selenide nanotubes could also be produced *via* other reaction mechanisms.[50] For example, the metal cations could be reduced by ethanol to produce metal atoms,[46,51] which then reacted with *t*-Se to produce a metal selenide sheath on the surface of each *t*-Se nanowire. By this mechanism, $RuSe_2$ (Fig. 3c) and $Pd_{17}Se_{15}$ nanotubes (Fig. 3d) have been synthesized in large quantities. In these cases, the

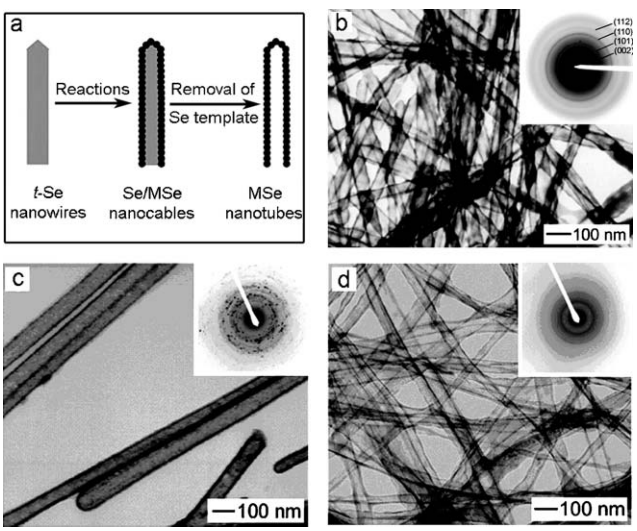

Fig. 3 (a) Schematic illustrating the formation of an Se–MSe nanocable and then an MSe nanotube by reacting *t*-Se nanowire with a metal salt, followed by removal of the unreacted core of *t*-Se. (b) TEM image of CdSe nanotubes that were prepared from the reaction between Cd^{2+} and Se^{2-} disproportionated from Se. The unreacted *t*-Se cores were removed by thermal evaporation. The inset shows a typical ED pattern. Adapted from ref. 48, © 2003 Wiley-VCH. Used with permission. TEM images of (c) $RuSe_2$ and (d) $Pd_{17}Se_{15}$ nanotubes that were synthesized from the reaction between *t*-Se nanowires and the metal, followed by removal of the unreacted *t*-Se template. The insets show their corresponding ED patterns. Adapted from ref. 50, © 2003 Elsevier. Used with permission.

wall thickness of resultant nanotubes was dependent on the concentration of metal salt, the reaction time, and the reaction temperature.

In the formation of both Pt and MSe nanotubes, the *t*-Se nanowires acted as both physical and chemical templates. The engagement of template in the nucleation step facilitates the initial formation of homogeneous, conformal coating on the template. This is also the major reason why *t*-Se was such a good template for the coating of metals when compared with inert structures such as polystyrene or silica, where complete coating by a metal is very hard to achieve without pretreating the surface with a primer bearing the appropriate functional group.[52] Furthermore, it was also recently demonstrated that the *t*-Se nanowires could be organized into ordered arrays such as networks (or meshes).[44,53] The approach described here is expected to play an increasingly important role in fabricating metal hollow nanostructures with complex (yet controllable) architectures.

Silver nanowires could also act as chemical template. We have shown that the galvanic replacement reaction between Ag nanowires and an aqueous $HAuCl_4$ solution could be used to produce pure Au and Au–Ag alloyed nanotubes with highly crystalline walls.[54] In this synthesis, the Ag nanowires served as both a source of electrons and shape scaffold, around which Au atoms were produced *in situ* through a redox process. Both microscopic and spectroscopic studies on this system revealed that the templating process proceeded through two distinctive steps. In the first step, due to a good matching between the lattice constants of Au and Ag, each Ag nanowire developed interior cavities (*i.e.*, tubular strips) and was then transformed into a nanotube with uniform sheath and smooth surface (Fig. 4a) made of a Au–Ag alloy through a combination of galvanic replacement reaction, alloying, and possibly Ostwald ripening. The second step involved the development of pores in the sheath through a dealloying process, in which silver atoms are selectively extracted from the alloyed wall to form pinholes in the surface (Fig. 4b). The tubular structure is complementary to the morphology of the Ag template, with the interior void determined by the dimension of the template. As shown in the inset of Fig. 4a, each tube had a pentagonal cross-section containing five straight side edges and five flat side surfaces, and all these features were essentially the same as the Ag nanowires. As alloying and dealloying was proceeding, the surface plasmon resonance (SPR) peaks of resultant nanotubes could be shifted from 380 nm to 930 nm.

The silver-engaged replacement reaction can, in principle, be extended to any metal whose redox potential is higher than that of the Ag^+/Ag pair. In addition to gold, we have examined Pt and Pd because the standard reduction potentials of these two metals are higher than that of Ag^+/Ag. From the TEM image of as-prepared Pt–Ag nanotubes (Fig. 4c), their walls seemed to be rougher and primarily composed of discrete nanoparticles. The difference between Au and Pt could be attributed to the lattice mismatch between Pt and Ag ($\sim$4.1%), which may prevent Pt atoms from growing epitaxially on the surface of silver. Fig. 4d shows an SEM image of Pd nanotubes prepared by reacting Ag nanowires with an aqueous solution of $Pd(NO_3)_2$, indicating that their surfaces were continuous and relatively smooth. Note that the precursor solution should

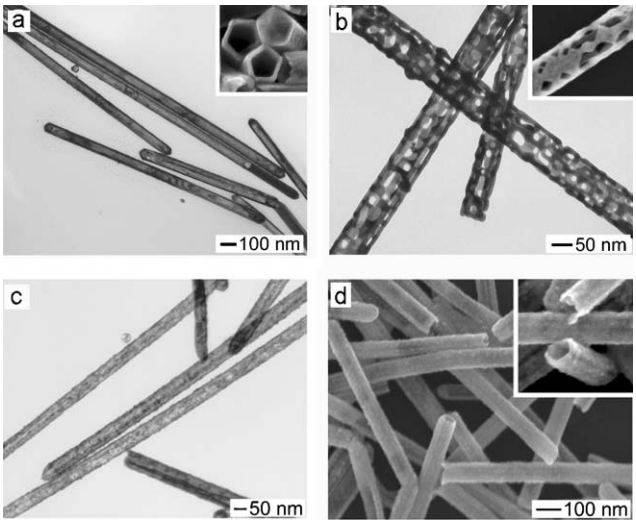

Fig. 4 (a) TEM images of Au–Ag alloyed nanotubes formed by reacting Ag nanowires with $HAuCl_4$. (b) TEM image of porous Au nanotubes formed by dealloying the Au–Ag nanotubes shown in (a). The insets are SEM images of the corresponding samples. Adapted from ref. 54*a*, © 2004 American Chemical Society. Used with permission. (c) Pt–Ag, and (d) Pd–Ag alloyed nanotubes prepared by reacting Ag nanowires with an aqueous solution of their salt precursor. The inset of (d) highlights an opening end of the nanotube. The walls of these nanotubes may also become porous when a dealloying process is applied. Adapted in part from ref. 54*b*, © 2003 Wiley-VCH. Used with permission.

be freshly prepared before each use, because the Pd cations would be hydrolyzed to form $Pd(OH)_2$ that was unable to oxidize Ag to Ag^+.

The galvanic replacement reaction can be further extended to fabricate multiple-walled nanotubes by combining with an electroless deposition process.[55] Fig. 5a schematically outlines all major steps that are required for fabrication of multiple-walled nanotubes composed of Au–Ag alloys. The first step is the formation of Au–Ag nanotubes with Ag nanowires as the template. The resultant nanotube is subsequently coated with a conformal, polycrystalline sheath of Ag *via* electroless plating. After the galvanic replacement reaction with $HAuCl_4$, a new tubular wall with slightly larger lateral dimensions is formed, and a double-walled nanotube is obtained. Coaxial nanotubes with more than two walls could be readily synthesized by repeating silver plating and galvanic replacement reaction. Fig. 5b and c show SEM images of double-walled and triple-walled Au–Ag alloyed nanotubes, respectively. From these images, it can be found that the multiple-walled nanotubes inherited all morphological details of the Ag template: *i.e.*, the five-fold, pentagonal cross-section with five straight edges and five flat side surfaces. This galvanic replacement reaction involving sacrificial silver templates could also be extended to fabricate hybrid nanotubes containing more than one metal. For example, we have successfully demonstrated fabrication of hybrid, double-walled nanotubes with outer and inner walls made of Pd–Ag and Au–Ag alloys, respectively, by reacting silver-plated Au–Ag nanotubes with an aqueous $Pd(NO_3)_2$ solution. Fig. 5d shows an SEM image of examples of this type of double-walled nanotube, revealing that the nanotubes made

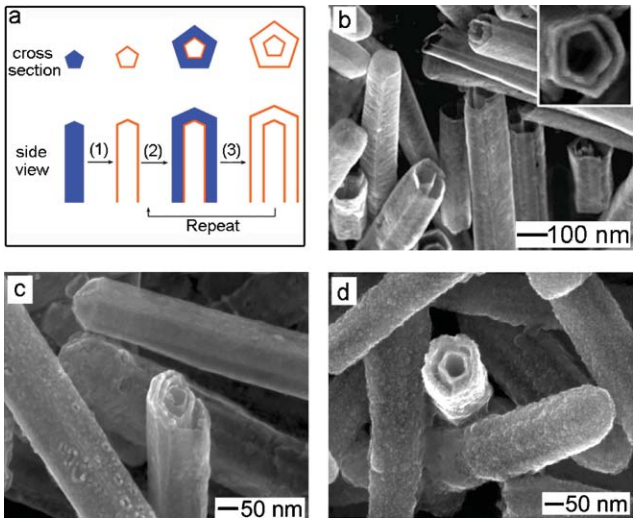

Fig. 5 (a) Schematic illustration of the experimental procedure used to fabricate metal nanotubes characterized by coaxial, multiple walls: (1), (3) template-engaged replacement reaction between Ag and $HAuCl_4$; (2) electroless plating of Ag. SEM images of (b) double-walled nanotubes made of Au–Ag alloys, (c) triple-walled nanotubes composed of Au–Ag alloys, and (d) double-walled nanotubes with the constituent material of the inner wall being Au–Ag alloy and the outer wall being Pd–Ag alloy. Adapted from ref. 55, © 2004 Wiley-VCH. Used with permission.

of Pd–Ag alloy were polycrystalline and mainly constructed from small nanoparticles. The poor crystallinity of the Pd–Ag alloy tubes might be related to the lattice mismatch between Pd and Ag, which caused the elemental Pd not to grow epitaxially on the surface of the electroplated silver (which was polycrystalline).

In general, the elemental composition and configuration of these core-sheath nanostructures are mainly determined by the starting template and the salt precursor participating in the replacement reaction. It is believed that this technique can be further extended to produce more complex nanostructures by incorporating more metals (or their alloys) into the synthetic scheme. These new tubular nanostructures made of metals and alloys are expected to find use in a range of applications. For example, computational studies suggested that the Au–Ag alloyed nanotubes with pentagonal cross sections might serve as good substrates for surface-enhanced Raman spectroscopic (SERS) detection of molecular species with ultrasensitivity in the spectral region from red to near-infrared, which happens to be a transparent window for soft tissues;[56] the polycrystalline Pd–Ag alloy tubes tend to have higher surface areas than their single-crystal counterparts and may exhibit greatly improved performance in catalysis.[57] To this end, the Pd–Ag nanotubes have been applied to effectively catalyze the Suzuki coupling reaction with yield approaching 100%.[58,54*b*]

Electrospinning technique

Electrospinning is a very simple and versatile technique for generating ultrathin fibers from various materials and on large scales.[59] The conventional setup for electrospinning includes a spinneret (usually a metallic needle), a syringe pump, a high-voltage power supply (DC or AC), and a grounded collector. In this technique, a polymer, sol-gel, or composite solution (as well as melt of a pure polymer) is loaded and then driven to the needle tip using a syringe pump, forming a droplet at the tip. As a high voltage is applied to the needle, the droplet becomes highly charged on its surface. Due to the repulsive interaction, the liquid droplet is elongated to form a Taylor cone and then stretched into an electrified jet. This jet will be continuously stretched by the electrostatic repulsion until the solvent has been evaporated or it is deposited on the grounded collector to form uniform fibers with nanoscale diameters.

Loscertales and his co-workers initially demonstrated a new design for the spinneret that contained two coaxial capillaries, and proposed to use it for the generation of a core-sheath jet consisting of two immiscible liquids.[60] Nevertheless, varicose break up of the electrified jet led to the formation of core-sheath particles. We and the Larsen group solved this problem by co-electrospinning two immiscible solutions, facilitated by cross-linking and thus stabilization of the sheath.[61] Core-sheath nanofibers with a broad range of diameters and sheath thicknesses could be fabricated using this setup. As illustrated by the design in Fig. 6, an ethanol solution containing a sol-gel precursor, a catalyst, and a polymer—typically titanium isopropoxide, acetic acid, and poly(vinyl pyrollidone) (PVP)—is loaded in the outer capillary while heavy mineral oil (which can be doped with additives) is added to the inner capillary. By judicially selecting the materials and their concentrations, one can achieve the correct viscosities and rates of hydrolysis and form a stable compound Taylor cone, leading to formation of a stable coaxial jet. Since a sol-gel precursor is added to the sheath solution, gelation in the outer surface of sheath during an electrospinning process can effectively prevent break up of the coaxial jet and thus enable

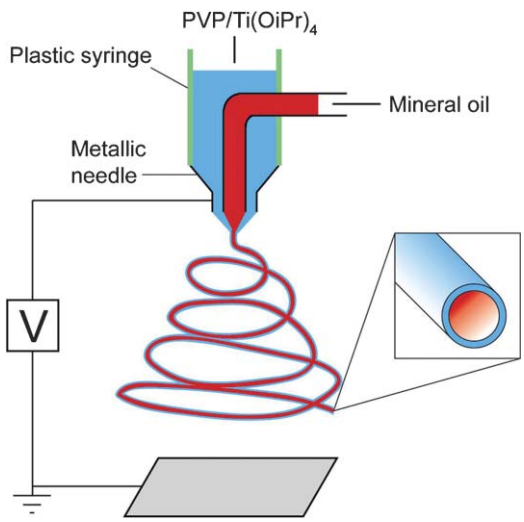

Fig. 6 Schematic illustration of the setup for electrospinning nanofibers with a core-sheath structure. The coaxial spinneret can be conveniently fabricated by inserting a silica capillary into a metallic needle. Heavy mineral oil and an ethanol solution containing PVP and $Ti(OiPr)_4$ were simultaneously ejected to form a continuous, coaxial jet. Adapted from ref. 61*a*, © 2004 American Chemical Society. Used with permission.

the formation of long, hollow fibers with uniform cross-sections.

For the system illustrated in Fig. 6, any molecular species soluble in the oil-phase can be directly incorporated into the nanofibers as they are electrospun from the coaxial spinneret. As an example, we used an amphiphilic fluorescent dye, 1,1′-dioctadecyl-3,3,3′,3′-tetramethylindocarbocyanine perchlorate ($DiIC_{18}$).[61b] Fig. 7a shows a fluorescence microscopy image of hollow fibers whose channels were filled with the $DiIC_{18}$-doped mineral oil. It is clear that the dye molecules were evenly distributed inside each hollow nanofiber. Most of the dye molecules were retained inside the fibers even after the oil-phase had been extracted with octane. It is believed that the dye molecules had been adsorbed onto the inner surfaces of the hollow fibers *via* interactions between their hydrophilic units and the hydroxy groups of titania. This method provides a simple procedure to load hollow nanostructures with various fluorescent dyes, as long as these dyes could be dissolved in the mineral oil. It also serves as a simple method to evaluate the uniformity of hollow fibers fabricated using this coaxial electrospinning technique.

The as-spun core-sheath nanofibers could be made hollow by extracting the mineral oil with a solvent such as octane, yielding long nanotubes whose walls are made of a titania–PVP composite. Further removal of PVP from the walls by calcination in air at 500 °C led to formation of polycrystalline anatase nanotubes (see Fig. 7b for a TEM image) with lengths up to hundreds of micrometers.[61a] Fig. 7c shows SEM images of another sample where the titania hollow nanofibers were collected as a uniaxially aligned array across the gap between two stripes of silicon substrates, followed by calcination in air. The inset shows an SEM image at a higher magnification, further confirming the formation of a tubular structure with circular cross-section and relatively smooth surfaces.

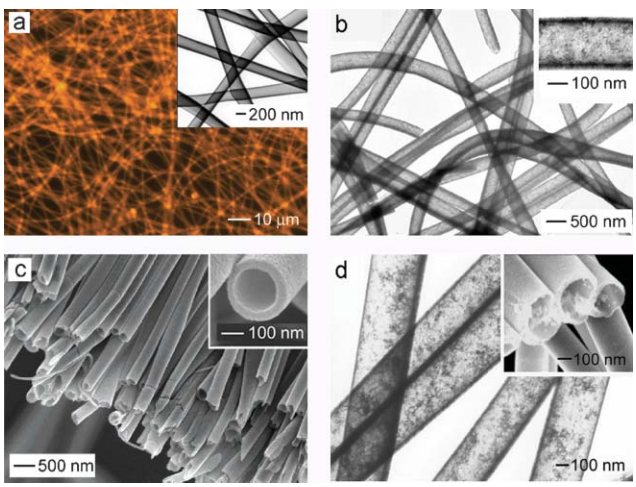

Fig. 7 (a) Fluorescence optical micrograph of hollow nanofibers whose inner surfaces were derivatized with the $DiIC_{18}$ dye. The inset shows a TEM image of these hollow fibers. (b) TEM image of TiO_2 (anatase) hollow fibers that were obtained by calcining the titania–PVP composite nanofibers in air at 500 °C. (c) SEM image of a uniaxially aligned array of anatase hollow fibers that were collected across the gap between a pair of electrodes. These fibers were then fractured using a sharp razor blade to expose their cross-sections. (d) TEM and SEM (inset) images of TiO_2 hollow fibers whose inner surfaces were selectively decorated with SnO_2 nanoparticles. This sample was prepared by co-electrospinning a mineral oil containing a tin alkoxide precursor (in the inner capillary) and an ethanol solution containing a titanium alkoxide (in the outer capillary), followed by calcination in air at 500 °C. Adapted from ref. 61*a*, © 2004 American Chemical Society and ref. 61*b*, © 2005 Wiley-VCH. Used with permission.

By modifying the oil core with different precursors, hollow nanofibers decorated with various functional species could be fabricated.[61b] For example, hollow nanofibers of titania filled with iron oxide nanoparticles were obtained by adding a dilute, oil-based ferrofluid to the core capillary, followed by extraction of the oil-phase with octane. The resultant hollow nanofibers were found to be magnetically active. By adding tin isopropoxide to the oil core, titania hollow nanofibers with tin oxide nanoparticles coated on their inner surfaces have also been successfully fabricated, as illustrated by the TEM and SEM images in Fig. 7d.

It is worth pointing out that the inner and outer surfaces of composite and ceramic hollow nanofibers could be selectively modified, and then exploited for use as catalyst supports, optical waveguides, and nanofluidic devices. Derivatizing the surfaces of these hollow nanofibers with different functional groups changes the surface chemistry, thereby allowing for the tuning of properties such as fluid flow rate, as well as the attachment of nanoparticles and other active compounds by chemical reaction with the functional groups. For instance, we have been able to selectively modify the inner and/or outer surfaces of the titania hollow nanofibers with oil-soluble, long-chain silanes.[61b]

Using the electrospinning method, a variety of new fibers with controllable core-sheath morphology could be fabricated by tuning the sol-gel mixtures. Furthermore, extension of the coaxial spinneret system to generate multi-walled nanofibers is technically feasible by adding more coaxial capillaries to the spinneret. Recently, several groups have demonstrated that core-sheath polymer nanofibers could also be fabricated by electrospinning two polymer solutions with miscible solvents using a coaxial spinneret. As future research is evolving, it is believed that electrospinning may become the technique of choice for fabricating long nanotubes with both inorganic and polymeric compositions.

Extension to other systems

The template-directed approach can also be applied to other types of nanostructures such as nanoparticles and spherical colloids. For instance, spherical colloids of *a*-Se with smooth surfaces and controllable sizes could be synthesized by using a solution-phase method based on the reduction of selenious acid with excessive hydrazine in ethylene glycol.[62] With *a*-Se colloids as a physical template, Se–Pt core-shell colloids have been synthesized. After removal of *a*-Se cores by soaking the sample in hydrazine, uniform Pt hollow spheres with smooth surfaces were obtained (see Fig. 8a for an SEM image).[45]

With *a*-Se colloidal spheres serving as chemical template, *a*-Se–Ag_2Se core-shell colloids (Fig. 8b) could be produced, in which $AgNO_3$ was reduced by ethylene glycol to generate Ag atoms that further reacted with *a*-Se to form monodispersed colloids consisting of *a*-Se cores and β-Ag_2Se shells.[63] The

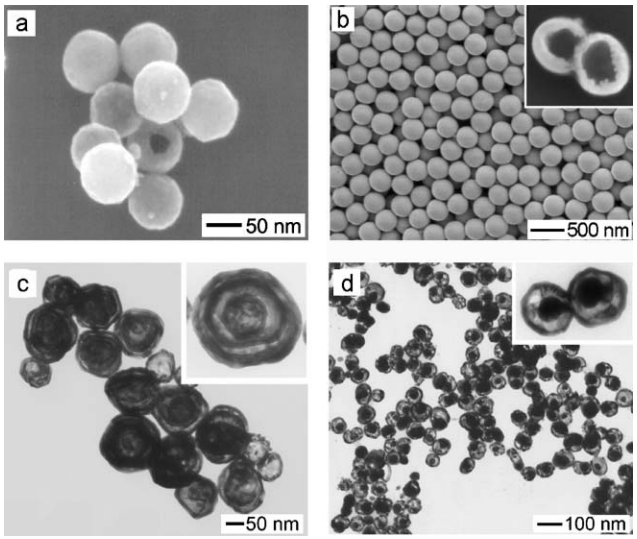

Fig. 8 (a) SEM image of Pt hollow spheres produced with *a*-Se as a template, followed by removal of the Se cores. Adapted in part from ref. 45, © 2003 American Chemical Society. Used with permission. (b) SEM image of Se–Ag_2Se core-shell colloids. The inset shows an SEM image of two broken colloids after the *a*-Se cores had been dissolved with hydrazine. Adapted in part from ref. 63, © 2005 Wiley-VCH. Used with permission. TEM images of (c) Au–Ag alloy nanoshells with triple walls and (d) Au–Ag alloy nanorattles that were prepared by using electroless plating and galvanic replacement reactions. Adapted in part from ref. 66, © 2004 American Chemical Society. Used with permission.

extent of conversion from *a*-Se to Ag_2Se could be controlled by adjusting the molar ratio of $AgNO_3$ to *a*-Se. Upon heating, the cores and shells changed phase from *a*-Se to *t*-Se and from β-Ag_2Se to α-Ag_2Se at 31 and 133 °C, respectively. When the Ag_2Se shells were sufficiently thick, the core-shell colloidal particles maintained their spherical shape while undergoing multiple cycles of phase transitions between β-Ag_2Se and α-Ag_2Se. This feature has been employed to fabricate photonic crystals with thermally switchable stop bands.[63] The core of *a*-Se could also be completely dissolved with hydrazine, which is clearly demonstrated by the SEM image of broken shells in the inset of Fig. 8b. Recent studies further demonstrated that Se–CdSe core-shell colloids could be obtained by exchanging the Ag^+ ions in Se–Ag_2Se colloids with Cd^{2+} in the presence of tributylphosphine (TBP) at 50 °C.[64] Such colloidal spheres with relatively high refractive indices could serve as a class of building blocks to fabricate photonic crystals with wide and strong stop bands.

The replacement reaction for generating Au–Ag alloyed nanotubes could be adopted to produce Au–Ag single-walled nanoshells, nanoboxes, and nanocages by replacing the Ag nanowires with nanospheres or nanocubes.[54] This extension has enabled us to prepare metal hollow nanostructures with controllable geometric shapes and structures, with their SPR peaks conveniently tunable in the spectral region from the visible to the near infrared (400–1200 nm). These SPR properties would lead to their applications in colorimetric sensing, nanoscale waveguiding, enhancement of electromagnetic fields and light transmission.[65] Using a procedure similar to the one used for the production of multi-walled Au–Ag alloyed nanotubes, we have also synthesized multi-walled nanoshells (or nanoscale Matrioshka, Fig. 8c), and nanorattles (Fig. 8d) by combining the electroless plating of Ag and the galvanic replacement reaction with $HAuCl_4$.[66] The specific nanostructures could be fabricated by controlling the sequence of Ag deposition and replacement reaction. It is interesting to note that the Au–Ag core encapsulated in each Au–Ag shell was movable if the nanorattles were immersed in a liquid medium. There are also a number of other interesting optical features associated with these new types of core-shell nanostructures of metals. For example, nanorattles made of Au–Ag alloys displayed two well-separated extinction peaks, a feature similar to that of Au or Ag nanorods. The peak at $\sim$510 nm could be attributed to the Au–Ag alloyed cores, while the other extinction peak at longer wavelength was associated with the Au–Ag shells and could be continuously tuned in the spectral range from the red to the near-infrared.

Potential applications

Like other inorganic nanotubes, the semiconductor and metal nanotubes fabricated using our methods are potentially useful in a range of applications, with possible examples including catalysis, photonics, electronics, optoelectronics, information storage, chemical and biological sensing, surface-enhanced Raman spectroscopy (SERS), and hydrogen storage. Here we only show one example related to the storage of hydrogen.

Pd–Ag alloy, the most commonly used system for hydrogen extraction in industry, has been demonstrated to exhibit the highest permeability for hydrogen at $\sim$23 wt% of Ag when measured at a pressure of 1 atm and temperature about 473 K.[67] It has also been shown by simulation that a further increase of Ag to higher concentrations (>63%) could lead to faster diffusion for hydrogen (as well as to lower material cost).[68] Furthermore, it has long been speculated that, when the grains of metals are reduced to the nanometre regime, they may exhibit significant improvement in hydrogen absorption behavior due to an increase in both surface area and grain boundaries. To this end, we produced Ag–(Pd–Ag) nanocables (Fig. 9a–9c) by refluxing Ag nanowires of about 20 μm in length and an aqueous $Pd(NO_3)_2$ solution.[69] In contrast to the case where short Ag nanowires (*e.g.*, <2 μm in length) yielded Pd nanotubes through the galvanic replacement reaction,[54] we found that only some segments of the long nanowires were converted into hollow structures. The total percentage of Ag in the final product was determined to be as high as 92.2 wt%. From the pressure–composition (PC) isotherms (Fig. 9d), it was found that the resultant nanostructures could exceed pure Pd powders or nanotubes in hydrogen solubility. The high solubility of hydrogen in the nanocable structures can be attributed to the formation of a thin sheath of Pd–Ag alloyed nanoparticles on the surface of each Ag nanowire. Because hydrogen is not soluble in pure silver, this sheath helped to split H_2 molecules into atoms, which could then diffuse into the lattice of silver.[70] This new system may provide a good model to investigate the adsorption and release of H_2 from metal nanostructures.

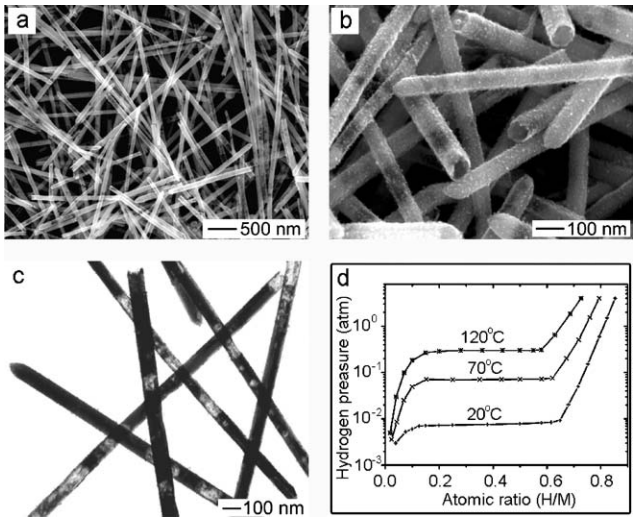

Fig. 9 (a, b) SEM images, and (c) TEM image of Ag nanowires whose surfaces had been coated with Pd–Ag alloyed sheaths. (d) PC isotherms for hydrogen desorption from the hydrides of as-synthesized Ag–(Pd–Ag) nanocables at 20, 70, and 120 °C. Here H/M is the hydrogen-to-metal ratio. Adapted from ref. 69, © 2004 American Chemical Society. Used with permission.

Summary and outlook

Nanotubes represent a new class of interesting and important nanostructures to study because of their superior performance in applications such as gas storage, energy conversion, fluid transportation, catalysis, electronics, optoelectronics, drug release, and sensing. The formation of tubular nanostructures generally requires the use of a layered or anisotropic crystal structure. There are reports of nanotubes made from materials that do not have a layered crystal structure, where they were synthesized by using carbon nanotubes and porous membranes as templates, or by rolling up thin films. In this feature article, we have demonstrated the versatility of some new approaches to the production of high quality nanotubes from a variety of inorganic solids, including both semiconductors and metals. These approaches can be grouped into three different clusters: concentration depletion at the surface of a seed, physical and chemical templating against both *t*-Se or Ag nanowires; and electrospinning with a coaxial capillary spinneret. Combined together, these approaches have greatly expanded the scope of inorganic materials that can be processed as nanotubes with uniform and controllable dimensions.

We believe that these techniques can be readily extended to produce more complex nanostructures with hollow interiors and cover a broader range of materials than those presented in this article by incorporating more reactions and thus more solid materials into the synthetic process. A good example will be the multi-walled tube systems discussed in the above sections. In general, by tailoring the composition, size, shape and/or structure of these nanotubes, one can control and fine-tune their properties to better-suit various applications. Since the capability and feasibility of these approaches have already been demonstrated to some extent, future work should be undertaken from the angle of a specific application rather than from the general desire of methodology development. In other words, future work in this area should be application-oriented. To this end, one should take advantage of the most effective procedure available, design and then synthesize or fabricate nanotubes with the desired property for a specific application.

Acknowledgements

This work has been supported in part by an AFOSR-MURI grant on smart skin materials awarded to the UW, a DARPA-DURINT subcontract from Harvard University, a fellowship from the David and Lucile Packard Foundation, the National Science Foundation (DMR-9983893, and DMR-0451788), and the Office of Naval Research (N00014-01-1-0976). Y. X. is an Alfred P. Sloan Research Fellow (2000–2005) and a Camille Dreyfus Teacher Scholar (2002–2007).

Notes and references

1 S. Iijima, *Nature*, 1991, **354**, 56.
2 (*a*) S. J. Tans, M. H. Devoret, H. Dai, A. Thess, R. E. Smalley, L. J. Geerligs and C. Dekker, *Nature*, 1997, **386**, 474; (*b*) H. Dai, J. H. Hafner, A. G. Rinzler, D. T. Colbert and R. E. Smalley, *Nature*, 1996, **384**, 147; (*c*) C. M. Lieber, *Solid State Commun.*, 1998, **107**, 607.
3 C. N. R. Rao, B. C. Satishkumar, A. Govindaraj and M. Nath, *ChemPhysChem*, 2001, **2**, 78.
4 (*a*) D. S. Bethune, C. H. Kiang, M. S. de Vries, G. Gorman, R. Savoy, J. Vazquez and R. Beyers, *Nature*, 1993, **363**, 605; (*b*) S. Iijima and T. Ichihashi, *Nature*, 1993, **363**, 603; (*c*) T. W. Ebbesen and P. M. Ajayan, *Nature*, 1992, **358**, 220.
5 (*a*) A. Thess, R. Lee, P. Nikolaev, H. Dai, P. Petit, J. Robert, C. Xu, Y. H. Lee, S. G. Kim, A. G. Rinzler, D. T. Colbert, G. E. Scuseria, D. Tománek, J. E. Fischer and R. E. Smalley, *Science*, 1996, **273**, 483; (*b*) H. Dai and A. G. Rinzler, *Chem. Phys. Lett.*, 1996, **260**, 471.
6 (*a*) Q. Fu, S. Huang and J. Liu, *J. Phys. Chem. B*, 2004, **108**, 6124; (*b*) H. M. Cheng, F. Li, G. Su, H. Y. Pan, L. L. He, X. Sun and M. S. Dresselhaus, *Appl. Phys. Lett.*, 1998, **72**, 3282; (*c*) M. Endo, K. Takeuchi, K. Kobori, K. Takahashi, H. W. Kroto and A. Sarkar, *Carbon*, 1995, **33**, 873; (*d*) S. Herreyre and P. Gadelle, *Carbon*, 1995, **33**, 234.
7 R. Tenne, *Angew. Chem., Int. Ed.*, 2003, **42**, 5124.
8 R. Tenne, L. Margulis, M. Genut and G. Hodes, *Nature*, 1992, **360**, 444.
9 Y. Feldman, E. Wasserman, D. J. Srolovitz and R. Tenne, *Science*, 1995, **267**, 222.
10 N. G. Chopra, R. G. Luyken, K. Cherrey, V. H. Crespi, M. L. Cohen, S. G. Louie and A. Zettl, *Science*, 1995, **269**, 966.
11 M. E. Spahr, P. Bitterli, R. Nesper, M. Müller, F. Krumeich and H. U. Nissen, *Angew. Chem., Int. Ed.*, 1998, **37**, 1263.
12 Y. R. Hacohen, E. Grunbaum, R. Tenne, J. Sloan and J. L. Hutchison, *Nature*, 1998, **395**, 337.
13 D. H. Galvan, J. H. Kim, M. B. Maple, M. Avalos-Berja and E. Adem, *Fullerene Sci. Technol.*, 2000, **8**, 143.
14 M. Nath and C. N. R. Rao, *Angew. Chem., Int. Ed.*, 2002, **41**, 3451.
15 M. Nath and C. N. R. Rao, *J. Am. Chem. Soc.*, 2001, **123**, 4841.
16 C. N. R. Rao and M. Nath, *Dalton Trans.*, 2003, 1.
17 O. G. Schmidt and K. Eberl, *Nature*, 2001, **410**, 168.
18 G. B. Saupe, C. C. Waraksa, H.-N. Kim, Y. J. Han, D. M. Kaschak, D. M. Skinner and T. E. Mallouk, *Chem. Mater.*, 2000, **12**, 1556.
19 (*a*) H. Nakamura and Y. Matsui, *J. Am. Chem. Soc.*, 1995, **117**, 2651; (*b*) P. Hoyer, *Langmuir*, 1996, **12**, 1411.
20 L. Pu, X. Bao, J. Zou and D. Feng, *Angew. Chem., Int. Ed.*, 2001, **40**, 1490.
21 B. Cheng and E. T. Samulski, *J. Mater. Chem.*, 2001, **11**, 2901.
22 J. Y. Li, X. L. Chen, Z. Y. Qiao, Y. G. Cao and H. Li, *J. Mater. Sci. Lett.*, 2001, **20**, 1987.
23 (*a*) Y. Xiong, Y. Xie, J. Yang, R. Zhang, C. Wu and G. Du, *J. Mater. Chem.*, 2002, **12**, 3712; (*b*) C. N. R. Rao, A. G. Govindaraj, F. L. Deepak, N. A. Gunari and M. Nath, *Appl. Phys. Lett.*, 2001, **78**, 1853.

24 L. Dloczik, R. Engelhardt, K. Ernst, S. Fiechter, I. Seiber and R. Könenkamp, *Appl. Phys. Lett.*, 2001, **78**, 3687.
25 J. C. Hutleen, K. B. Jirage and C. R. Martin, *J. Am. Chem. Soc.*, 1998, **120**, 6603.
26 G. Tourillon, L. Pontonnier, J. P. Levy and V. Langlais, *Electrochem. Solid-State Lett.*, 2000, **3**, 20.
27 E. Matijević, *Langmuir*, 1994, **10**, 8.
28 J. Aizenberg, A. J. Black and G. M. Whitesides, *Nature*, 1999, **398**, 495.
29 (*a*) G. C. Krueger and C. W. Miller, *J. Chem. Phys.*, 1953, **21**, 2018; (*b*) A.-L. Barabasi and H. E. Stanley, *Fractal Concepts in Surface Growth*, Cambridge University Press, Cambridge, 1995.
30 B. Mayers and Y. Xia, *Adv. Mater.*, 2002, **14**, 279.
31 P. Day, *Solid State Chemistry Compounds*, ed. A. K. Cheetham and P. Day, Clarendon Press, Oxford, 1992, ch. 3.
32 (*a*) Y. R. Ma, L. M. Qi, J. M. Ma and H. M. Cheng, *Adv. Mater.*, 2004, **16**, 1023; (*b*) X. M. Li, Y. Li, S. Q. Li, W. W. Zhou, H. B. Chu, W. Chen, I. L. Li and Z. K. Tang, *Cryst. Growth Des.*, 2005, **5**, 911; (*c*) H. Zhang, D. R. Yang, Y. J. Ji, X. Y. Ma, J. Xu and D. L. Que, *J. Phys. Chem. B*, 2004, **108**, 1179.
33 J. Yang, Y. C. Liu, H. M. Liu and C. C. Chen, *Adv. Mater.*, 2004, **16**, 713.
34 Y. Xia, P. Yang, Y. Wu, B. Mayers, B. Gates, Y. Yin, F. Kim and H. Yan, *Adv. Mater.*, 2003, **15**, 353.
35 R. R. He, M. Law, R. Fan, F. Kim and P. Yang, *Nano Lett.*, 2002, **2**, 1109.
36 (*a*) L. J. Lauhon, M. S. Gudiksen, D. Wang and C. M. Lieber, *Nature*, 2002, **420**, 57; (*b*) Y. Zhang, K. Suenaga, C. Colliex and S. Iijima, *Science*, 1998, **281**, 973.
37 (*a*) S. O. Obare, N. R. Jana and C. J. Murphy, *Nano Lett.*, 2001, **1**, 601; (*b*) K. S. Mayya, D. I. Gittins, A. M. Dibaj and F. Caruso, *Nano Lett.*, 2001, **1**, 727.
38 (*a*) H. Dai, E. W. Wong, Y. Z. Lu, S. Fan and C. M. Lieber, *Nature*, 1995, **375**, 769; (*b*) Y. Zhang and H. Dai, *Appl. Phys. Lett.*, 2000, **77**, 3015; (*c*) Y. Zhang, N. W. Franklin, R. J. Chen and H. Dai, *Chem. Phys. Lett.*, 2000, **331**, 35; (*d*) P. M. Ajayan, O. Stephan, P. Redlich and C. Colliex, *Nature*, 1995, **375**, 564; (*e*) C. Tang, S. Fan, M. L. de la Chapelle, H. Dang and P. Li, *Adv. Mater.*, 2000, **12**, 1346; (*f*) J. Zhu and S. Fan, *J. Mater. Res.*, 1999, **14**, 1175; (*g*) C. N. R. Rao, B. C. Satishkumar and A. Govindaraj, *Chem. Commun.*, 1997, 1581; (*h*) Y. Wu, B. Messer and P. Yang, *Adv. Mater.*, 2001, **13**, 1487; (*i*) J. H. Song, Y. Wu, B. Messer, H. Kind and P. Yang, *J. Am. Chem. Soc.*, 2001, **123**, 10397.
39 (*a*) Y. Sun, B. Gates, B. Mayers and Y. Xia, *Nano Lett.*, 2002, **2**, 165; (*b*) Y. Sun and Y. Xia, *Adv. Mater.*, 2002, **14**, 833.
40 (*a*) W. Stöber, A. Fink and E. Bohn, *J. Colloid Interface Sci.*, 1968, **26**, 62; (*b*) M. Ocana, W. P. Hsu and E. Matijević, *Langmuir*, 1991, **7**, 2911; (*c*) W. P. Hsu, R. Yu and E. Matijević, *J. Colloid Interface Sci.*, 1993, **156**, 56; (*d*) R. E. Partch, Y. Xie, S. T. Oyama and E. Matijević, *J. Mater. Res.*, 1993, **8**, 2014; (*e*) Y. Lu, Y. Yin, B. T. Mayers and Y. Xia, *Nano Lett.*, 2002, **2**, 183.
41 (*a*) M. Ohmori and E. Matuevic, *J. Colloid Interface Sci.*, 1992, **150**, 594; (*b*) L. M. Liz-Marzán, M. Giersig and P. Mulvaney, *Chem. Commun.*, 1996, 731; (*c*) L. M. Liz-Marzán, M. Giersig and P. Mulvaney, *Langmuir*, 1996, **12**, 4329; (*d*) S. O. Obare, N. R. Jana and C. J. Murphy, *Nano Lett.*, 2001, **1**, 601.
42 Y. Yin, Y. Lu, Y. Sun and Y. Xia, *Nano Lett.*, 2002, **2**, 427.
43 (*a*) H. Nakamura and Y. Matsui, *J. Am. Chem. Soc.*, 1995, **117**, 2651; (*b*) H. Nakamura and Y. Matsui, *Adv. Mater.*, 1995, **7**, 871; (*c*) C. N. R. Rao, B. C. Satishkumar and A. Govindaraj, *Chem. Commun.*, 1997, 1581; (*d*) R. A. Caruso, J. H. Schattka and A. Greiner, *Adv. Mater.*, 2001, **13**, 1577.
44 (*a*) B. Mayers, K. Liu, D. Sunderland and Y. Xia, *Chem. Mater.*, 2003, **15**, 3852; (*b*) B. Gates, B. T. Mayers, A. Grossman and Y. Xia, *Adv. Mater.*, 2002, **14**, 1749; (*c*) B. Gates, Y. Yin and Y. Xia, *J. Am. Chem. Soc.*, 2000, **122**, 12582; (*d*) B. Gates, B. Mayers, B. Cattle and Y. Xia, *Adv. Funct. Mater.*, 2002, **12**, 219.
45 B. Mayers, X. Jiang, D. Sunderland, B. Cattle and Y. Xia, *J. Am. Chem. Soc.*, 2003, **125**, 13364.
46 D. M. Chizhikov and V. P. Shchastlivyi, *Selenium and Selenides*, (translated from the Russian by E. M. Elkin), Collet's LTD, London, 1968, p. 40.
47 (*a*) H. Hirai, *J. Macromol. Sci., Chem.*, 1979, **A13**, 633; (*b*) T. Teranishi, M. Hosoe and M. Miyake, *Adv. Mater.*, 1997, **9**, 65.
48 X. Jiang, B. Mayers, T. Herricks and Y. Xia, *Adv. Mater.*, 2003, **15**, 1740.
49 (*a*) D. M. Chizhikov and V. P. Shchastlivyi, *Selenium and Selenides*, (translated from the Russian by E. M. Elkin), Collet's LTD, London, 1968, p. 39; (*b*) C. Wang, W. Zhang, X. Qian, X. Zhang, Y. Xie and Y. Qian, *Mater. Chem. Phys.*, 1999, **60**, 99; (*c*) Q. Peng, Y. Dong and Y. Li, *Inorg. Chem.*, 2002, **41**, 5249.
50 X. Jiang, B. Mayers, Y. Wang, B. Cattle and Y. Xia, *Chem. Phys. Lett.*, 2003, **15**, 1740.
51 T. Teranishi, M. Hosoe and M. Miyake, *Adv. Mater.*, 1997, **9**, 65.
52 (*a*) S. J. Oldenburg, R. D. Averitt, S. L. Westcott and N. J. Halas, *Chem. Phys. Lett.*, 1998, **288**, 243; (*b*) F. Caruso, M. Spasova, V. Salgueiriño-Maceira and L. M. Liz-Marzán, *Adv. Mater.*, 2001, **13**, 1090.
53 X. Cao, Y. Xie and L. Li, *Adv. Mater.*, 2003, **15**, 1914.
54 (*a*) Y. Sun and Y. Xia, *J. Am. Chem. Soc.*, 2004, **126**, 3892; (*b*) Y. Sun, B. Mayers and Y. Xia, *Adv. Mater.*, 2003, **15**, 641.
55 Y. Sun and Y. Xia, *Adv. Mater.*, 2004, **16**, 264.
56 J. P. Kottmann, O. J. F. Martin, D. R. Smith and S. Schultz, *Phys. Rev. B: Condens. Matter Mater. Phys.*, 2001, **64**, 235402.
57 S.-W. Kim, M. Kim, W. Y. Lee and T. Hyeon, *J. Am. Chem. Soc.*, 2002, **124**, 7642.
58 (*a*) Y. Li, X. M. Hong, D. M. Collard and M. A. El-Sayed, *Org. Lett.*, 2000, **2**, 2385; (*b*) M. T. Reetz, R. Breinbauer and K. Wanninger, *Tetrahedron Lett.*, 1996, **37**, 4499.
59 (*a*) A. Formalas, *U. S. patent*, 1 975 504, 1934; (*b*) J. Doshi and D. H. Reneker, *J. Electrost.*, 1995, **35**, 151; (*c*) D. H. Reneker and I. Chun, *Nanotechnology*, 1996, **7**, 216; (*d*) A. Theron, E. Zussman and A. L. Yarin, *Nanotechnology*, 2001, **12**, 384; (*e*) G. Larsen, R. Spretz and R. Velarde-Ortiz, *Adv. Mater.*, 2004, **16**, 166.
60 G. Loscertales, A. Barrero, I. Guerrero, R. Cortijo, M. Marquez and A. M. Gañán-Calvo, *Science*, 2002, **295**, 1695.
61 (*a*) D. Li and Y. Xia, *Nano Lett.*, 2004, **4**, 933; (*b*) D. Li, J. T. McCann and Y. Xia, *Small*, 2005, **1**, 83; (*c*) G. Larsen, R. Velarde-Ortiz, K. Minchow, A. Barrero and I. G. Loscertales, *J. Am. Chem. Soc.*, 2003, **125**, 1154.
62 U. Jeong and Y. Xia, *Adv. Mater.*, 2005, **17**, 102.
63 U. Jeong and Y. Xia, *Angew. Chem., Int. Ed.*, 2005, **44**, 3099.
64 U. Jeong, J. U. Kim, Y. Xia and Z.-Y. Li, *Nano Lett.*, 2005, **5**, 937.
65 Y. Xia and N. J. Halas, *MRS Bull.*, 2005, **30**, 338.
66 Y. Sun, B. Wiley, Z.-Y. Li and Y. Xia, *J. Am. Chem. Soc.*, 2004, **126**, 9399.
67 (*a*) A. Weiss, S. Ramaprabhu and N. Rajalakshmi, *Z. Phys. Chem.*, 1997, **199**, 165; (*b*) S. Uemiya, T. Matsuda and E. Kikuchi, *J. Membr. Sci.*, 1991, **56**, 315.
68 H. Barlag, L. Opara and H. Züchner, *J. Alloys Compd.*, 2002, **330**, 434.
69 Y. Sun, Z. Tao, J. Chen, T. Herricks and Y. Xia, *J. Am. Chem. Soc.*, 2004, **126**, 5940.
70 O. M. Løvvik and R. A. Olsen, *J. Alloys Compd.*, 2002, **330–332**, 332.

